JOURNAL OF NEUROTRAUMA 33:1202–1211 (July 1, 2016)

DOI: 10.1089/neu.2015.4067

Time Course and Size of Blood–Brain Barrier Opening in a Mouse Model of Blast-Induced Traumatic Brain Injury

Christopher D. Hue,[1] Frances S. Cho,[1] Siqi Cao,[1] Russell E. Nicholls,[2] Edward W. Vogel III,[1] Cosmas Sibindi,[1] Ottavio Arancio,[2] Cameron R. "Dale" Bass,[3] David F. Meaney,[4] and Barclay Morrison III[1]

Abstract

An increasing number of studies have reported blood–brain barrier (BBB) dysfunction after blast-induced traumatic brain injury (bTBI). Despite this evidence, there is limited quantitative understanding of the extent of BBB opening and the time course of damage after blast injury. In addition, many studies do not report kinematic parameters of head motion, making it difficult to separate contributions of primary and tertiary blast-loading. Detailed characterization of blast-induced BBB damage may hold important implications for serum constituents that may potentially cross the compromised barrier and contribute to neurotoxicity, neuroinflammation, and persistent neurologic deficits. Using an *in vivo* bTBI model, systemic administration of sodium fluorescein (NaFl; 376 Da), Evans blue (EB; 69 kDa when bound to serum albumin), and dextrans (3-500 kDa) was used to estimate the pore size of BBB opening and the time required for recovery. Exposure to blast with 272 ± 6 kPa peak overpressure, 0.69 ± 0.01 ms duration, and 65 ± 1 kPa*ms impulse resulted in significant acute extravasation of NaFl, 3 kDa dextran, and EB. However, there was no significant acute extravasation of 70 kDa or 500 kDa dextrans, and minimal to no extravasation of NaFl, dextrans, or EB 1 day after exposure. This study presents a detailed analysis of the time course and pore size of BBB opening after bTBI, supported by a characterization of kinematic parameters associated with blast-induced head motion.

Key words: blast injury; blood–brain barrier; dextran; shock tube; traumatic brain injury

Introduction

There have been over 300,000 medical diagnoses of traumatic brain injury (TBI) among United States Armed Forces alone, which have been largely attributed to blast exposure in recent military conflicts in Iraq and Afghanistan.[1,2] The exact biophysical determinants of blast-induced TBI (bTBI) are still an area of active investigation, but an increasing number of studies assert that the direct interaction with blast overpressure (i.e., a shock wave) is sufficient to cause damage to the brain and blood–brain barrier (BBB).[3–9] Clinical observations of patients who have sustained bTBI confirm the frequent occurrence of brain edema, vasospasm, and intracranial hemorrhage, implicating insult to the neurovascular unit.[1,2,10,11] Traumatic cerebral vasospasm has been reported to last for up to 30 days in patients with moderate-to-severe bTBI.[10,11] Microhemorrhage may cause glial scarring and white matter degeneration, which may be linked to chronic traumatic encephalopathy (CTE), vascular dementia, and Alzheimer's disease.[12,13] Therefore, damage to the BBB may be a major hallmark of bTBI that initiates secondary injury mechanisms and symptoms related to cerebrovascular dysfunction, emphasizing that the loss of BBB integrity may be a clinically important facilitator of the pathophysiology of blast injury.[1,3,7,8,14]

The rapidly growing body of experimental evidence *in vivo* and *in vitro* supports that BBB breakdown is a characteristic outcome of blast exposure,[4,7,8,15] and in some cases, of pure primary blast injury.[3,5,6,9,16,17] In murine models of bTBI, BBB opening has been assessed most frequently by extravasation of Evans blue (EB)[3,7,15] and immunoglobulin G (IgG).[4,8,9,16] Recent reports suggest that the loss of restrictive barrier properties is mediated by reduced expression or pathological reorganization of tight junction proteins including zonula occludens (ZO)-1, claudin-5, and occludin.[3,5,6,15,17] It is important to note, however, that others also have reported inconsistent BBB damage despite efforts to precisely control blast injury parameters,[4,8,16] as evidenced in one study by negligible BBB breakdown in approximately half of injured animals.[16] Together, this evidence points to the complexity of BBB breakdown after blast injury, which may be further confounded by

[1]Department of Biomedical Engineering, Columbia University, New York, New York.
[2]Taub Institute for Research on Alzheimer's Disease and the Aging Brain, Columbia University, New York, New York.
[3]Department of Biomedical Engineering, Duke University, Durham, North Carolina.
[4]Department of Bioengineering, University of Pennsylvania, Philadelphia, Pennsylvania.

the variety of loading regimes and biomechanical injury parameters (peak overpressure, duration, and impulse) used in different studies.

To help shed necessary insight on the extent of BBB disruption after blast injury, we characterized the pore size of BBB opening and its time course for spontaneous recovery after exposure to blast injury by measuring extravasation of sodium fluorescein (NaFl), EB, and dextrans of distinct molecular masses (3, 70, and 500 kDa). We utilized a previously described *in vivo* blast injury model with high-speed video to control and report the biomechanics of injury and minimize head motion associated with blast exposure.[18,19] We report that BBB opening was sufficient to permit significant extravasation of molecules less than approximately 70 kDa in the acute period after blast, with recovery of BBB integrity by 1 day post-injury. This study is the first to characterize the time course and pore size of BBB opening after blast exposure, and holds important implications for the influx of serum constituents into the brain that may initiate secondary pathological cascades after bTBI.

Methods

Animal preparation

All experiments using mice were conducted in accordance with animal welfare guidelines established by the Institutional Animal Care and Use Committee of Columbia University. Wild-type adult mice (male and female, 10–14 weeks old, 20–30 g), were a filial 1 hybrid of C57BL/6 mice obtained from The Jackson Laboratory (Bar Harbor, ME) and 129SvEv mice obtained from Taconic (Germantown, NY). A total of 103 animals were used for this study and divided among sham and injured groups for NaFl, three different-size dextrans (3, 70, and 500 kDa), and EB at each post-injury time-point (Days 0 and 1).

In vivo *blast-induced traumatic brain injury model*

Our bTBI model consisted of a 76 mm-diameter shock tube that was previously described in detail,[18] with a 25 mm-length driver section pressurized with helium gas and a 1240 mm-long driven section.[20] The body of the mouse was secured within a rigid pipe to protect the torso but expose the head 15 mm away from the shock tube exit where the shock wave is still nearly planar (Fig. 1).[18–20] The head was further restrained using an adjustable, metal nose bar to minimize motion of the head during blast exposure. Pressure transducers (Endevco 8530B-1000; Meggitt Sensing Systems, Irvine, CA) were flush-mounted at the shock tube exit, as well as inside the mouse holder in close proximity to the animal torso.[18]

Exposure to blast and administration of tracers

Prior to blast exposure, animals were anesthetized with isoflurane (Henry Schein Animal Health, Dublin, OH) until completely secured and oriented in the custom mouse holder. Animals were then exposed to a single blast. Animal cohorts were injected by tail vein either immediately prior to blast (Day 0) or 1 day post-blast with different tracers. Sham controls were processed identically to injured animals but were not exposed to blast.

Tracers of different molecular masses were used to determine blast-induced BBB opening. For NaFl, animals received 4 μL/g of a 10% solution of NaFl (376 Da) dissolved in phosphate-buffered saline (PBS).[21] For biotinylated dextrans (Life Technologies, Carlsbad, CA), each animal received 0.16 mg/g of dextran (3, 70, or 500 kDa) dissolved in PBS. The hydrodynamic diameters (DH) were previously determined by dynamic light scattering: 3 kDa (D7135; DH $\sim$2 nm), 70 kDa (D1957; DH $\sim$10 nm), 500 kDa (D7142; DH $\sim$30 nm).[22,23] For EB, animals received 4 μL/g of a 2% solution of EB (69 kDa when bound to serum albumin) dissolved in PBS.[21]

Tissue preparation and ex vivo fluorescence imaging and analysis

Animals were perfusion-fixed 4 h after administration of tracers. Animals were perfused with PBS for 6 min at 21 mL/min to remove tracers from the vasculature, followed by perfusion fixation with

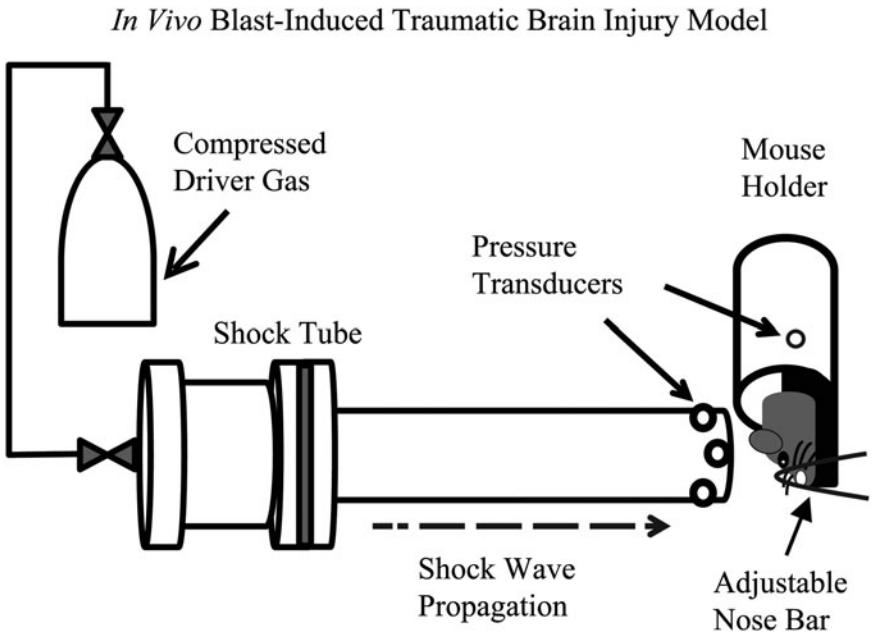

FIG. 1. *In vivo* blast-induced traumatic brain injury model consisting of a shock tube and custom-designed mouse holder.[18] Pressure transducers were flush-mounted at the exit of the tube and within the mouse holder. The mouse head was aligned 15 mm away from the exit of the tube. An adjustable nose bar was used to restrain the mouse head and minimize head motion during blast exposure. Figure not drawn to scale.

4% paraformaldehyde (PFA; dissolved in PBS) for 6 min at 21 mL/min. Brains were then extracted and sliced using a vibrating blade microtome (Vibratome 1000 Plus; Leica Biosystems, St. Louis, MO). A total of 10 coronal sections (labeled S1–S10), each 1 mm-thick, were cut from every brain, excluding the olfactory bulbs and brain stem. Brain samples containing biotinylated dextrans were fluorescently labeled during a 1 h incubation with a 1:100 dilution (in PBS) of streptavidin-Alexa Fluor® 647 conjugate (S32357; Life Technologies). All fluorescently-labeled dextran brain sections (Ex: 650 nm/Em: 668 nm), EB brain sections (Ex: 540 nm/Em: 680 nm), and NaFl brain sections (Ex: 440 nm/Em: 525 nm) were imaged using a CRi Maestro 2 Imaging System (Perkin Elmer, Waltham, MA). A custom image analysis script was developed using MATLAB (R2014b; MathWorks, Natick, MA) to automate detection of the individual area in pixels and mean fluorescence intensity of each brain section.

High-speed video analysis

A Phantom v4.2 high-speed camera (Vision Research, Wayne, NJ) was used to record a frontal view of head motion associated with blast exposure. Videos were acquired at a resolution of 256×256 and a frame rate of 7407 frames per second. Similar to our previous publication,[18] a custom image processing script was developed using MATLAB (MathWorks) to track changes in eye position to quantify head kinematics (displacement, velocity, and acceleration) over time.

Confocal microscopy

High-resolution fluorescence images of EB-labeled sections were captured using a Leica TCS SP5 laser scanning confocal microscope equipped with a Leica HI Plan 4 x, 0.10 numerical aperture dry objective and a DMI6000 B inverted microscope (Leica Microsystems, Wetzlar, Germany). Brain sections were imaged with a helium-neon 543 nm laser, and emitted light was captured at a range of 620 nm-700 nm. A total of 12 tile-scan images per section were acquired at a resolution of 1024×1024 with a scanning speed of 10 Hz, and were stitched together using Leica Application Suite software (Leica Microsystems) to generate a composite image of a complete coronal section.

Statistical analysis

All data are presented as mean ± standard error of the mean. Statistical significance was determined using one-way analysis of variance (ANOVA) to compare the mean fluorescence intensity of NaFl, EB, and dextrans (3, 70, 500 kDa) between corresponding sham and injured brain sections. Statistical comparisons also were performed for each time-point after blast injury (SPSS v. 22; IBM, Armonk, NY; $p < 0.05$).

Results

Kinematic analysis of blast-induced head motion

Animals were exposed to a shock wave with a 272 ± 6 kPa peak overpressure, 0.69 ± 0.01 ms duration, and 65 ± 1 kPa*ms impulse. Consistent with our previous study,[18] head motion generally was characterized by rapid head movement in the direction parallel to the incident shock wave, followed by a slower and prolonged movement in the reverse direction, and a slow lateral evolution of the head as it reached its final position. The peak displacement, velocity, and acceleration of the head all were dramatically greater in the direction parallel to the incident shock wave (x component) than in the perpendicular direction (y component; Table 1). Blast-induced head motion of a representative mouse, using head restraint, is presented in Fig. 2. The peak pressure measured inside of the animal holder, adjacent to the torso, was 24 ± 1 kPa, which was well below reported thresholds for pulmonary injury.[24] We also note that after injury, we did not observe any gross macroscopic pulmonary injury (data not shown).[18]

Table 1. Kinematic Analysis of Head Motion[a]

	Displacement (m)	*Velocity (m/s)*	*Acceleration (m/s^2)*
Maximum total	0.003 ± 0.0001	7.07 ± 0.33	16349 ± 819
Maximum X	0.003 ± 0.0001	6.93 ± 0.33	16493 ± 819
Maximum Y	0.001 ± 0.0001	1.75 ± 0.10	6977 ± 380

[a]Mean ± standard error of the mean; $n = 20$ independent high-speed videos of mouse blast exposure.

Blast-induced blood-brain barrier opening

In contrast to sham controls, blast resulted in widespread extravasation of NaFl and 3 kDa dextran in the acute period (Day 0) after exposure (Fig. 3A, 3B). EB also was visible in several injured brain sections in the acute period after exposure, when compared with EB-injected sham animals (Fig. 3C). However, there was no qualitative indication of extravasation of the 70 or 500 kDa dextrans acutely after injury except for scattered localized regions of fluorescence (Fig. 3D, 3E). At 1 day after blast exposure, there were no visible differences in extravasation of the different-size dextrans or EB between injured and sham samples (Fig. 4A–4D), suggesting that the BBB had recovered. Qualitatively, as the molecular mass increased, accumulation of dextran in injured samples was less widespread.

Quantification of blast-induced blood-brain barrier opening

Quantitative analysis of the mean fluorescence intensity of each brain section confirmed qualitative visual trends. The mean fluorescence intensity of NaFl was significantly increased in the acute

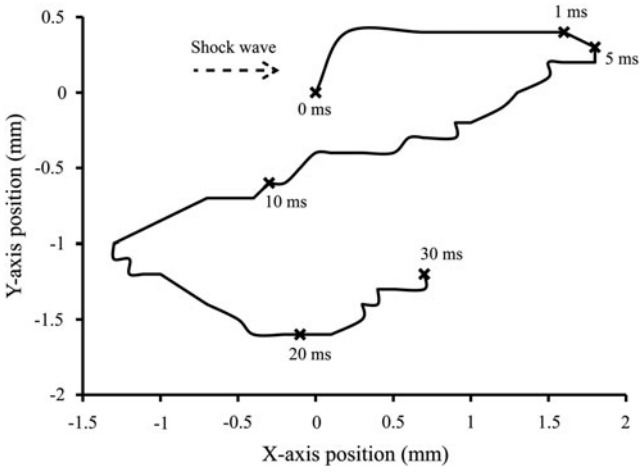

FIG. 2. Head motion induced by blast exposure for a representative mouse (with head restraint). After blast exposure, the mouse head returned to rest at 31 ms. The direction of the oncoming shock wave is represented by the dashed arrow.

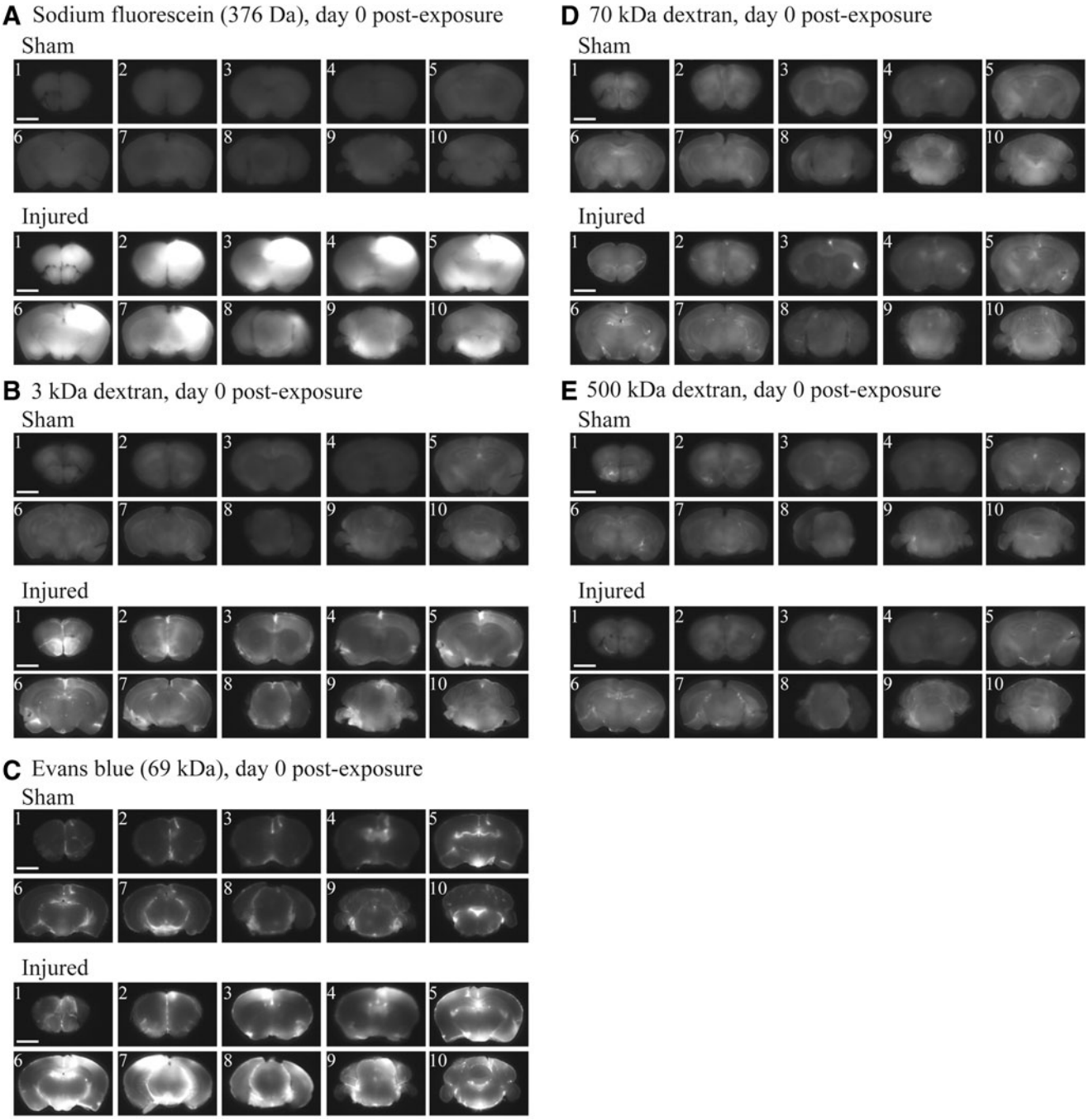

FIG. 3. Blood–brain barrier opening in the acute post-injury period (Day 0). Sections from a representative sham or injured brain are presented for each tracer. **(A)** Strong, widespread fluorescence of sodium fluorescein throughout the entire blast-injured brain on Day 0. **(B)** Widespread fluorescence of 3 kDa dextran throughout the entire blast-injured brain on Day 0. **(C)** Regions of strong Evans blue fluorescence in several injured brain sections on Day 0. **(D, E)** No qualitative differences in fluorescence of 70 or 500 kDa dextrans between sham and injured brains on Day 0. Scale bar = 3 mm.

period after exposure (Day 0) in all injured brain sections (Fig. 5A). The mean fluorescence intensity of 3 kDa dextran was significantly increased in the acute period after exposure (Day 0) in all injured brain sections except in section 10 (S10; $p = 0.061$; Fig. 5B). Mean fluorescence intensity of EB also was significantly greater in injured brain sections 3, 7, and 8 (S3, S7, and S8) in the acute period after blast (Fig. 5C). Fluorescence intensity of 70 or 500 kDa dextrans was not altered in the acute post-injury period (Fig. 5D, 5E). At 1 day after blast exposure, mean fluorescence intensity was unaltered for NaFl and only significantly higher in injured samples in section 4 (S4) for 3 kDa dextran, section 3 (S3) for EB, and section 6 (S6) for 70 kDa dextran (Fig. 6A–6D). The quantitative results support that blast-induced BBB opening permits the influx of molecules less than approximately 70 kDa in the acute post-injury period, with spontaneous recovery of the BBB 1 day after exposure.

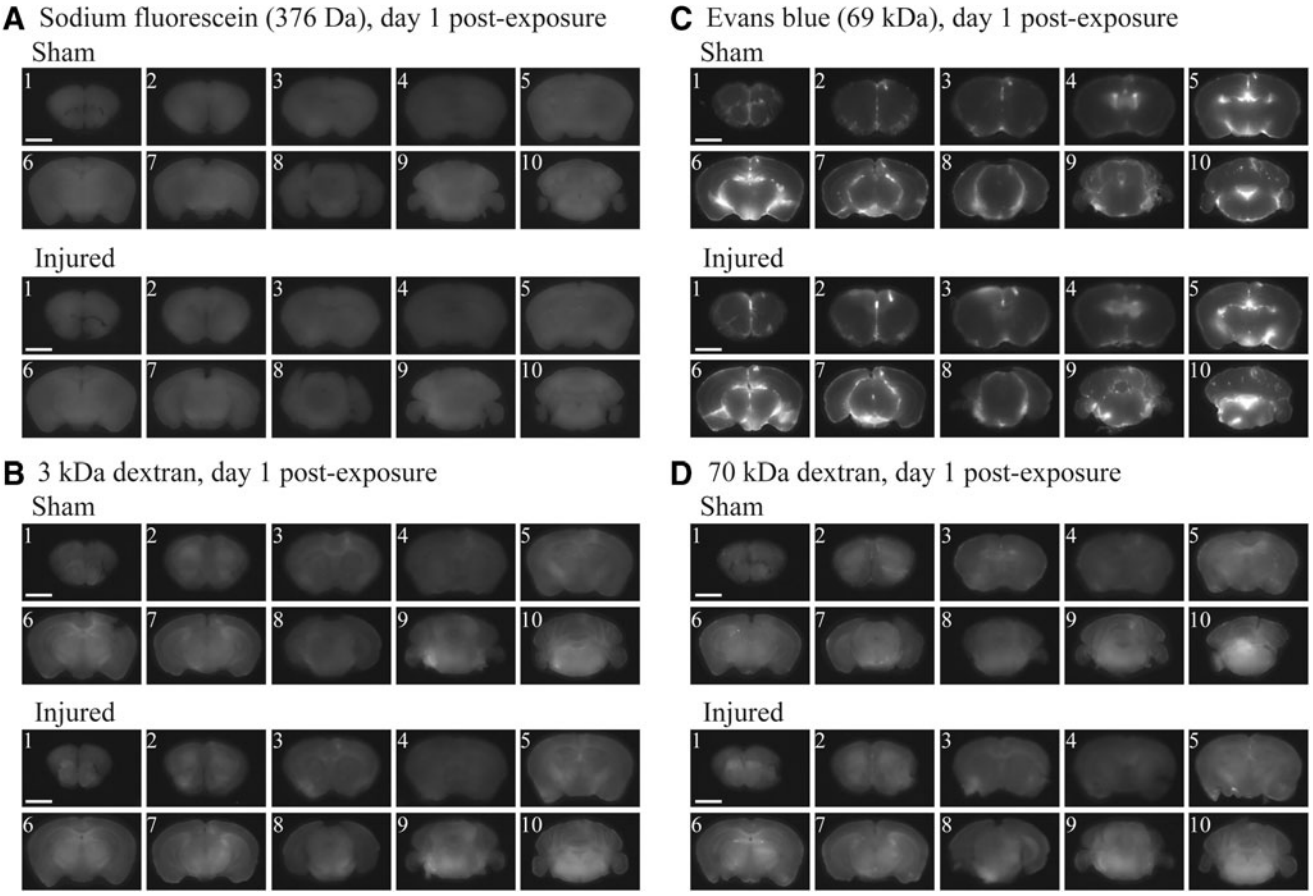

FIG. 4. Blood-brain barrier opening 1 day post-injury. Sections from a representative sham or injured brain are presented for each tracer. **(A, B, C, D)** No qualitative differences in fluorescence of sodium fluorescein, 3 or 70 kDa dextrans, or Evans blue on Day 1 after injury. Scale bar = 3 mm.

Microscopic evaluation of blood-brain barrier damage after blast

In the acute period (Day 0) after sham exposure, there were no regions of EB fluorescence indicative of any BBB disruption in a representative sham sample, as determined by high-resolution confocal microscopy (section 5; −1.6 mm from bregma; Fig. 7A). By contrast, there was widespread EB fluorescence throughout a corresponding blast-injured brain section that appeared to be strongest in the right motor (MO) and somatosensory cortex (SS), as well as in the left piriform (PIR), entorhinal (ENT), and perirhinal (PERI) cortex (Fig. 7B). Although specific anatomical regions of EB extravasation and fluorescence intensity varied across injured samples, overall BBB breakdown appeared to be diffuse but strongest in the cerebral cortex, which was consistent with previous findings.[4,7,8,15]

Discussion

This study reports a detailed characterization of BBB opening and recovery time course after blast injury using a range of different-sized tracers. We report the recovery of BBB function 1 day after blast exposure in mice, which is in close agreement with a recent *in vivo* bTBI study.[7] In previous reports, acute opening of the BBB after blast, as demonstrated by EB extravasation, persisted for at least 6 h after injury, with recovery of barrier integrity by 24 h.[7,15] This time course of blast-induced BBB dysfunction is also in overall agreement with non-blast models of TBI, in which BBB opening occurs transiently and returns to control levels within hours to a few days.[4–6,8,25,26] Based on findings in our current study, significant differences in mean intensity between sham and injured animals for NaFl, 3 kDa dextran, and EB on Day 0 were dramatically reduced by Day 1 after injury, providing evidence to support the recovery of BBB integrity 1 day after blast exposure at our loading conditions. The qualitative pattern of dextran fluorescence after blast exposure (Fig. 3B) was similar to that reported in previous studies of BBB opening induced by focused ultrasound.[22,23] We also recognize that other small tracers and imaging techniques may provide potentially greater sensitivity for detecting small defects in the damaged BBB after TBI, such as gadolinium and magnetic resonance imaging.[27]

Our data suggest that molecules smaller than approximately 70 kDa can penetrate the BBB in the acute period after blast injury at conditions tested in our study, but are excluded by 1 day after exposure when the BBB has recovered. However, other studies have reported the extravasation of larger molecules such as IgG (160 kDa)[26] after blast injury.[4,8,9,16] Differences in the apparent pore size of blast-induced BBB opening between our findings and those of other studies may be attributed to the variety of injury parameters tested (peak overpressure, duration, impulse, head acceleration). It is unclear exactly which biomechanical parameter(s) most strongly contribute to BBB opening *in vivo*, but a number of

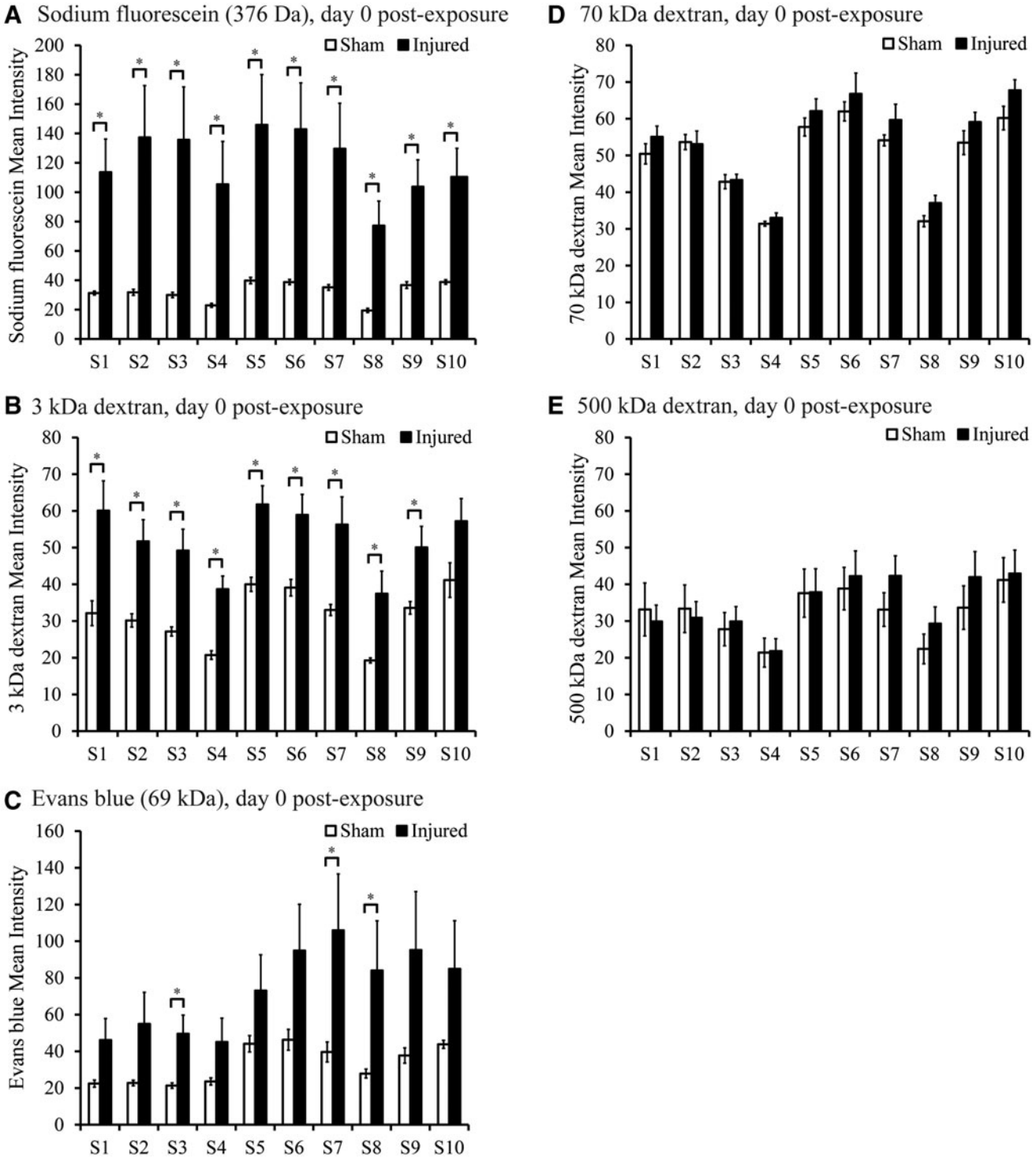

FIG. 5. Quantification of blood-brain barrier opening in the acute post-injury period (Day 0). **(A)** Mean fluorescence intensity of sodium fluorescein significantly increased throughout injured brain sections after blast exposure on Day 0 ($n \geq 3$ animals per exposure condition). **(B)** Mean fluorescence intensity of 3 kDa dextran significantly increased throughout injured brain sections after blast exposure on Day 0 ($n = 7$ animals per exposure condition). **(C)** Mean fluorescence intensity of Evans blue significantly increased in several injured brain sections (S3, S7, and S8) after blast exposure on Day 0 ($n \geq 6$ animals per exposure condition). **(D, E)** No changes in fluorescence of 70 or 500 kDa dextrans after injury on Day 0 ($n \geq 5$ animals per dextran tracer and exposure condition). $^*p < 0.05$; ± standard error of the mean. S1–S10, brain sections.

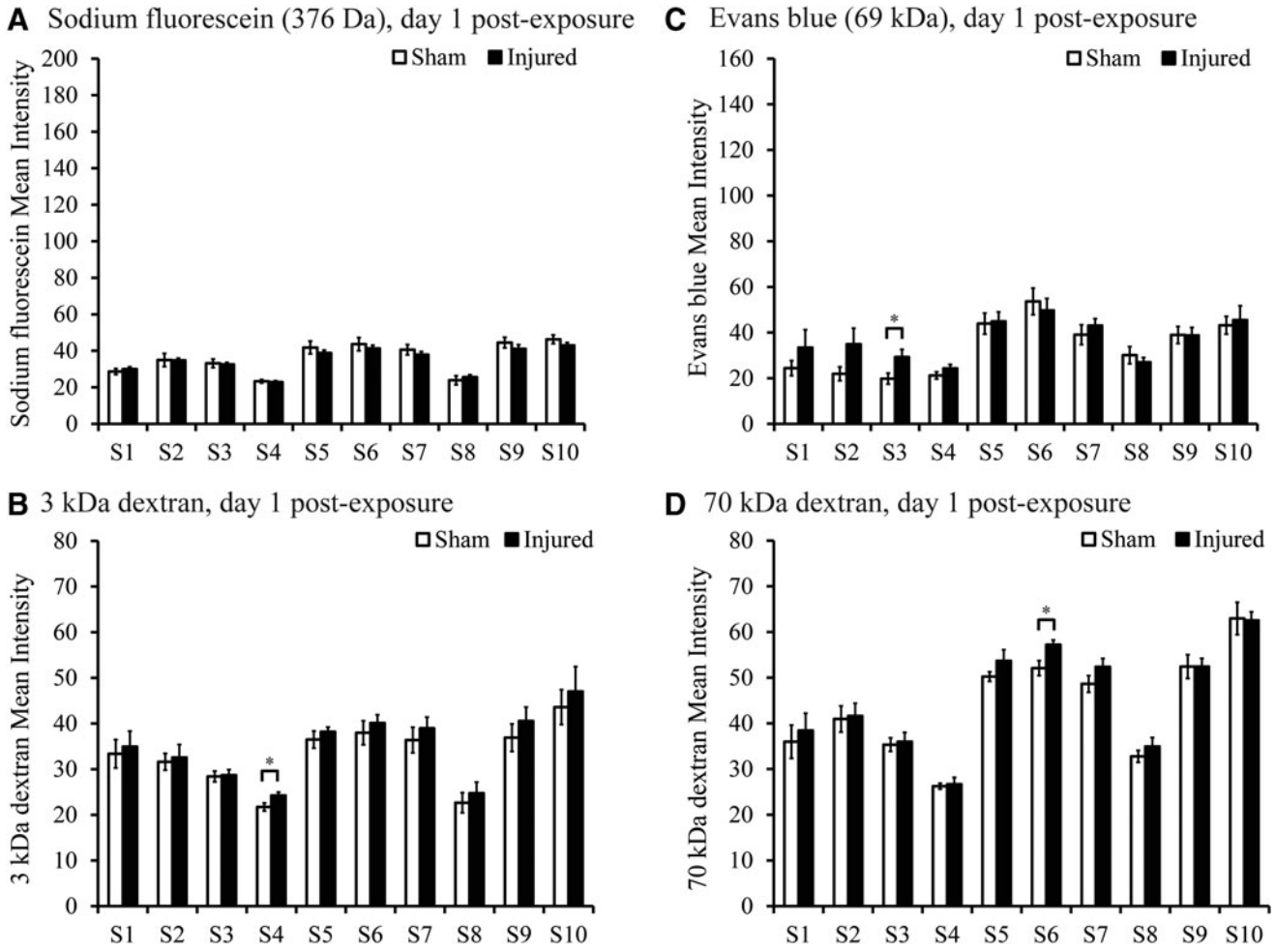

FIG. 6. Quantification of blood–brain barrier opening 1 day post-injury. **(A, B, C, D)** Minimal to no differences in mean fluorescence intensity of sodium fluorescein ($n \geq 3$ animals per exposure condition), 3 and 70 kDa dextrans ($n = 6$ animals per dextran tracer and exposure condition), and Evans blue (EB; $n = 6$ animals per exposure condition) on Day 1 after blast exposure, strongly supporting the recovery of BBB integrity. $*p < 0.05$; ± standard error of the mean. S1–S10, brain sections.

studies exposed animals to longer overpressure durations,[4,8,16] others tested similar or greater overpressures,[9] and some may have potentially allowed higher head accelerations without having quantified blast-induced head motion.[4,8,28] Because IgG (and other proteins) are endogenously present in serum, unlike exogenous tracers such as dextran, NaFl, and EB that are rapidly cleared from systemic circulation,[29,30] more IgG may accumulate in the brain for a given defect, thereby improving the limit of detection for BBB breakdown.

Potential disparities in the time course of BBB breakdown that currently exist in the bTBI literature may also be related to variations in the biomechanics of different blast injury models. For example, exposure to primary blast injury (confirming the absence of head motion) at a range of different overpressure levels resulted in widespread IgG staining 24 h after injury but was only present in approximately half of all animals tested at a given blast level.[16] Focal lesions scattered throughout the brain also were observed by IgG staining after primary blast injury in rats.[9] Another study of primary blast injury reported significant extravasation of EB and NaFl in rats 24 h after exposure to a shock wave with a 123 kPa overpressure and estimated 4 ms duration,[3] which was longer than that tested in our study. Other studies suggested that IgG immunoreactivity in the brain was present 24 h after blast exposure, and was reduced to control levels by 3 days.[4,8] However, because head accelerations were typically not measured in these studies, it is difficult to quantify contributions of inertial-driven (i.e., tertiary) injury in addition to blast overpressure (i.e., primary blast) when interpreting BBB breakdown. Although we only tested one exposure level in the current study, we have reported mouse head accelerations and shock wave parameters to more fully describe our blast conditions and enable more direct comparisons with future studies (Table 1).

Angular acceleration of the head (without blast exposure) has been postulated to result in widespread pathological and morphological changes to the cerebrovasculature throughout the brain.[31] Controlled angular head accelerations of approximately $1–2 \times 10^5$ rad/s^2 resulted in extravasation of blood from vessels throughout the brain as well as subdural and intracerebral hematomas in non-human primates.[31–34] Rapid rotation of the piglet head with peak angular accelerations of approximately $1.0–1.5 \times 10^5$ rad/s^2 caused subarachnoid bleeding and accumulation of blood in ventricles and the brain parenchyma, without overt BBB disruption as determined by IgG staining.[35] Rotational head acceleration of 2.1×10^5 rad/s^2 in rabbits also resulted in severe subarachnoid hemorrhage, focal intracerebral

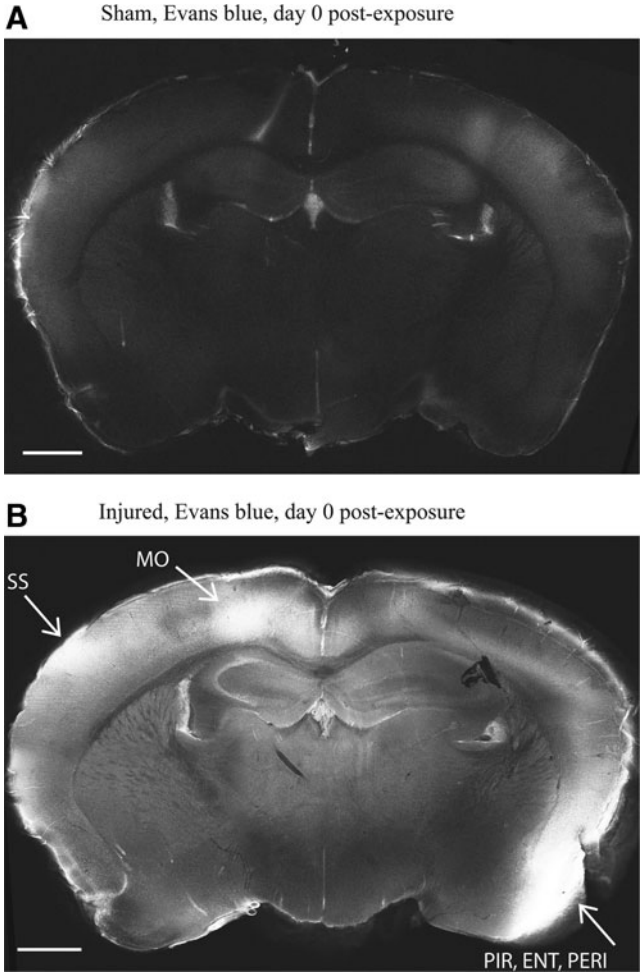

FIG. 7. Confocal microscopy of Evans blue (EB) fluorescence in the acute period (Day 0) after blast exposure. **(A)** No regions of strong EB fluorescence in sham exposed brain section. **(B)** Widespread EB fluorescence indicating blood–brain barrier (BBB) breakdown in an example injured brain section, with strongest regions of fluorescence in the right motor (MO) and somatosensory (SS) cortex, as well as in the left piriform (PIR), entorhinal (ENT), and perirhinal (PERI) cortex (white arrows). Anatomical regions of BBB damage as well as fluorescence intensity varied across injured samples, but were generally strongest in the cerebral cortex. Scale bar = 1 mm.

bleeding, and reactive astrogliosis, potentially causing damage to the BBB.[36] Rotational head trauma of approximately $3.7–10.0 \times 10^5$ rad/s^2 in rats resulted in damage to blood vessels, subarachnoid hemorrhage, and intraparenchymal lesions,[37,38] which was further supported in one study by the release of S100B proteins from brain glial cells into the serum.[37] After blast exposure in mice, Goldstein and colleagues[39] reported peak average angular head acceleration of 9.54×10^5 rad/s^2, which was associated with microvascular pathology and abnormal BBB ultrastructure. In our current bTBI study, peak angular head acceleration associated with BBB opening was estimated to be 7×10^5 rad/s^2 (peak linear acceleration of 16,349 m/s^2; Table 1), within the range of head accelerations reported in non-blast and blast models of TBI.

We have previously demonstrated that restraining head motion, protecting the torso, and modifying the orientation can influence animal survival and neurological deficits after blast exposure.[18] Reduction of head acceleration by using effective head restraint promoted animal survival.[18] In addition, protecting the torso significantly reduced mortality in rats exposed to blast.[40,41] Others have previously noted the importance of head accelerations on the neurological deficits and pathological consequences of blast injury.[39,41] Although our careful efforts to restrain the head did reduce overall motion, accelerations remained appreciable (Table 1). However, improved mouse survival with the use of head restraint enabled us to study the effects of relatively high blast overpressures, compared with the range tested in related bTBI studies.[3,4,7–9,15,16] Our results also highlight a more general challenge in interpreting the effects of blast in the majority of *in vivo* bTBI models, in which inertial contributions of head motion can be minimized but not completely eliminated.

A number of studies describing cerebrovascular compromise after blast injury report the diffuse nature of BBB breakdown. In some cases, damage in general anatomical regions was observed, revealing diffuse staining predominantly in the prefrontal and outer layers of the cortex,[4,7,8,15,16] and minimal to no staining in the brainstem and cerebellum.[4] Consistent with these previous findings, overall BBB breakdown observed in the current study was widespread and diffuse, but generally strongest in the cerebral cortex under microscopic evaluation (Fig. 7). Others have reported non-region specific focal lesions, determined by IgG staining, that were present throughout the brain and grew larger in size and number after exposure to increasingly more severe primary blast injuries.[9] That particular primary blast study exposed animals to overpressures comparable to or greater than our study, but with much shorter durations on the order of microseconds.[9] Although our findings share general observations of BBB breakdown with previous bTBI studies, there is little current evidence to suggest that specific anatomical brain regions are preferentially susceptible to BBB damage after blast injury.

BBB opening lasting up to 24 h after blast exposure, as supported by our results, has been associated with neurovascular inflammation, widespread microglial activation, astrocyte reactivity, abnormal endothelial ultrastructure, and neuronal degeneration.[3,4,8,39] These pathological biochemical and cellular processes may cause long-lasting detrimental effects despite apparent BBB recovery occurring as quickly as 1 day after blast. For instance, microglial activation in the hippocampus and substantia nigra have been detected 5–10 days after blast exposure[8] and in the superficial layers of the cerebral and cerebellar cortex for up to 14 days after blast injury in rats.[42] Others have hypothesized that free radicals, hydrogen peroxide, and peroxynitrite released from activated microglia contribute to subsequent oxidative damage and neurodegeneration.[8] BBB breakdown after traumatic insult has been reported to result in the influx of serum factors such as albumin, fibrinogen, and thrombin, which together may contribute to microglial activation, oxidative stress, and the release of proinflammatory mediators in the brain.[43–45] Our results of BBB opening hold implications for similar pathological extravasation of blood-borne components that might occur after blast. Ultimately, oxidative injury and neuroinflammation related to blast-induced BBB disruption may be key contributors to prolonged neurological deficits after bTBI. Studies also suggest that blast exposure may result in minimal acute neuronal degeneration, but may trigger delayed cell death through apoptotic cascades related to brain microvascular dysfunction.[3,7,46,47] Future work is warranted to determine if BBB opening after blast is a critical initiator to these secondary injury mechanisms, or only worsens ongoing pathological processes.

Although we focused on characterizing the duration and pore size of BBB opening, future studies will investigate associated secondary injury mechanisms and if the potential infiltration of serum components contributes to longer-term blast-related sequelae. Abdul-Muneer and colleagues[3] reported that acute mechanical insult due to shock wave exposure triggered oxidative and nitrosative stress responses involving activation of NADPH oxidase 1 (NOX-1) and inducible nitric oxide synthase (iNOS), matrix metalloproteinases (MMP-2, -3, -9), and water channel aquaporin-4 (AQP4), ultimately exacerbating BBB damage, edema, and neuroinflammation.[3] Diffuse cerebral edema is a prominent pathophysiologic feature in the acute period of bTBI that contributes to neurologic decline, and is thought to be closely related to cerebrovascular compromise.[2,11,48] These pathological signaling mechanisms may contribute to cognitive and behavioral deficits after blast injury.[1,7,14,49] Despite the fact that BBB breakdown is a transient phenomenon that is repaired within days, barrier compromise may be linked to a number of alternative signaling pathways that can result in long-term pathological effects.[5–8] Lucke-Wold and colleagues[15] have suggested that blast-induced alterations in the activity of different isozymes of protein kinase C (PKC), including PKCα, PKCδ, and PKCε, directly influence cerebrovascular function.[15] PKCα may regulate localization and function of tight junction proteins ZO-1 and occludin, PKCδ may affect vascular tone, and PKCε may confer neuroprotection after traumatic insult.[15] Blast-induced BBB damage has also been associated with accumulation of intracellular Ca^{2+} due to cellular membrane compromise, triggering endoplasmic reticulum stress, the unfolded protein response, and apoptosis.[7,50] Taken together, neuroinflammation, the endoplasmic reticulum stress response, and PKC activity are all important secondary injury mechanisms after blast exposure that may be influenced by concomitant BBB dysfunction.[3,7,8,15]

In conclusion, we have determined the time course and pore size of BBB opening after blast-loading conditions tested in the current study by measuring extravasation of tracers with distinct molecular masses (376 Da-500 kDa). BBB opening in the acute period after blast injury permitted significant extravasation of molecules smaller than approximately 70 kDa, followed by recovery of BBB integrity by 1 day post-injury. This study supports the hypothesis that transient opening of the BBB may permit serum components to infiltrate the brain parenchyma, initiating secondary pathological cascades that can persist long after recovery of the BBB, suggesting that BBB repair may be a therapeutic strategy to pursue in future studies.

Acknowledgments

This work was supported by a Multidisciplinary University Research Initiative from the U.S. Army Research Office (B.M., D.F.M., C.R.B.; W911MF–10–1–0526), the U.S. Army Medical Research and Materiel Command (O.A.; W81XWH-12-1-0579), and a National Science Foundation Graduate Research Fellowship (C.D.H.; DGE–07–07425). The authors would like to acknowledge Gwen B. Effgen for helpful discussions and insightful suggestions pertaining to experimental design and development of the blast injury model.

Author Disclosure Statement

No competing financial interests exist.

References

1. Chen, Y., Huang, W., and Constantini, S. (2013). Concepts and strategies for clinical management of blast-induced traumatic brain injury and posttraumatic stress disorder. J. Neuropsychiatry Clin. Neurosci. 25, 103–110.
2. Magnuson, J., Leonessa, F., and Ling, G.S. (2012). Neuropathology of explosive blast traumatic brain injury. Curr. Neurol. Neurosci. Rep. 12, 570–579.
3. Abdul-Muneer, P.M., Schuetz, H., Wang, F., Skotak, M., Jones, J., Gorantla, S., Zimmerman, M.C., Chandra, N., and Haorah, J. (2013). Induction of oxidative and nitrosative damage leads to cerebrovascular inflammation in an animal model of mild traumatic brain injury induced by primary blast. Free Radic. Biol. Med. 60, 282–291.
4. Garman, R.H., Jenkins, L.W., Switzer, R.C., Bauman, R.A., Tong, L.C., Swauger, P.V., Parks, S.A., Ritzel, D.V., Dixon, C.E., Clark, R.S.B., Bayır, H., Kagan, V., Jackson, E.K., and Kochanek, P.M. (2011). Blast exposure in rats with body shielding is characterized primarily by diffuse axonal injury. J. Neurotrauma 28, 947–959.
5. Hue, C.D., Cao, S., Dale Bass, C.R., Meaney, D.F., and Morrison, B., 3rd. (2014). Repeated primary blast injury causes delayed recovery, but not additive disruption, in an in vitro blood-brain barrier model. J. Neurotrauma 31, 951–960.
6. Hue, C.D., Cao, S., Haider, S.F., Vo, K.V., Effgen, G.B., Vogel, E., 3rd, Panzer, M.B., Bass, C.R., Meaney, D.F., and Morrison, B., 3rd. (2013). Blood-brain barrier dysfunction after primary blast injury in vitro. J. Neurotrauma 30, 1652–1663.
7. Logsdon, A.F., Turner, R.C., Lucke-Wold, B.P., Robson, M.J., Naser, Z.J., Smith, K.E., Matsumoto, R.R., Huber, J.D., and Rosen, C.L. (2014). Altering endoplasmic reticulum stress in a model of blast-induced traumatic brain injury controls cellular fate and ameliorates neuropsychiatric symptoms. Front. Cell. Neurosci. 8, 421.
8. Readnower, R.D., Chavko, M., Adeeb, S., Conroy, M.D., Pauly, J.R., McCarron, R.M., and Sullivan, P.G. (2010). Increase in blood-brain barrier permeability, oxidative stress, and activated microglia in a rat model of blast-induced traumatic brain injury. J. Neurosci. Res. 88, 3530–3539.
9. Yeoh, S., Bell, E.D., and Monson, K.L. (2013). Distribution of blood-brain barrier disruption in primary blast injury. Ann. Biomed. Eng. 41, 2206–2214.
10. Armonda, R.A., Bell, R.S., Vo, A.H., Ling, G., DeGraba, T.J., Crandall, B., Ecklund, J., and Campbell, W.W. (2006). Wartime traumatic cerebral vasospasm: recent review of combat casualties. Neurosurgery 59, 1215–1225.
11. Ling, G., Bandak, F., Armonda, R., Grant, G., and Ecklund, J. (2009). Explosive blast neurotrauma. J. Neurotrauma 26, 815–825.
12. Glushakova, O.Y., Johnson, D., and Hayes, R.L. (2014). Delayed increases in microvascular pathology after experimental traumatic brain injury are associated with prolonged inflammation, blood-brain barrier disruption, and progressive white matter damage. J. Neurotrauma 31, 1180–1193.
13. Wu, J., Pajoohesh-Ganji, A., Stoica, B.A., Dinizo, M., Guanciale, K., and Faden, A.I. (2012). Delayed expression of cell cycle proteins contributes to astroglial scar formation and chronic inflammation after rat spinal cord contusion. J. Neuroinflammation 9, 169.
14. Chen, Y. and Huang, W. (2011). Non-impact, blast-induced mild TBI and PTSD: concepts and caveats. Brain Inj. 25, 641–650.
15. Lucke-Wold, B.P., Logsdon, A.F., Smith, K.E., Turner, R.C., Alkon, D.L., Tan, Z., Naser, Z.J., Knotts, C.M., Huber, J.D., and Rosen, C.L. (2014). Bryostatin-1 restores blood brain barrier integrity following blast-induced traumatic brain injury. Mol. Neurobiol. 52, 1119–1134.
16. Skotak, M., Wang, F., Alai, A., Holmberg, A., Harris, S., Switzer, R.C., and Chandra, N. (2013). Rat injury model under controlled field-relevant primary blast conditions: acute response to a wide range of peak overpressures. J. Neurotrauma 30, 1147–1160.
17. Hue, C.D., Cho, F.S., Cao, S., Dale Bass, C.R., Meaney, D.F., and Morrison, B. III. (2015). Dexamethasone potentiates in vitro blood-brain barrier recovery after primary blast injury by glucocorticoid receptor-mediated upregulation of ZO-1 tight junction protein. J. Cereb. Blood Flow Metab. 35, 1191–1198.
18. Gullotti, D.M., Beamer, M., Panzer, M.B., Chen, Y.C., Patel, T.P., Yu, A., Jaumard, N., Winkelstein, B., Bass, C.R., Morrison, B., and Meaney, D.F. (2014). Significant head accelerations can influence immediate neurological impairments in a murine model of blast-induced traumatic brain injury. J. Biomech. Eng. 136, 091004.
19. Patel, T.P., Gullotti, D.M., Hernandez, P., O'Brien, W.T., Capehart, B.P., Morrison, B., 3rd, Bass, C., Eberwine, J.E., Abel, T., and Meaney, D.F. (2014). An open-source toolbox for automated phenotyping of mice in behavioral tasks. Front. Behav. Neurosci. 8, 349.
20. Panzer, M.B., Matthews, K.A., Yu, A.W., Morrison, B., 3rd, Meaney, D.F., and Bass, C.R. (2012). A multiscale approach to blast neuro-

trauma modeling: part I—development of novel test devices for in vivo and in vitro blast injury models. Front. Neurol. 3, 46.
21. Yen, L.F., Wei, V.C., Kuo, E.Y., and Lai, T.W. (2013). Distinct patterns of cerebral extravasation by Evans blue and sodium fluorescein in rats. PLoS One 8, e68595.
22. Chen, H. and Konofagou, E.E. (2014). The size of blood-brain barrier opening induced by focused ultrasound is dictated by the acoustic pressure. J. Cereb. Blood Flow Metab. 34, 1197–1204.
23. Choi, J.J., Wang, S., Tung, Y.S., Morrison, B., 3rd, and Konofagou, E.E. (2010). Molecules of various pharmacologically-relevant sizes can cross the ultrasound-induced blood-brain barrier opening in vivo. Ultrasound Med. Biol. 36, 58–67.
24. Bass, C.R., Rafaels, K.A., and Salzar, R.S. (2008). Pulmonary injury risk assessment for short-duration blasts. J. Trauma 65, 604–615.
25. Enters, E.K., Pascua, J.R., McDowell, K.P., Kapasi, M.Z., Povlishock, J.T., and Robinson, S.E. (1992). Blockade of acute hypertensive response does not prevent changes in behavior or in CSF acetylcholine (ACH) content following traumatic brain injury (TBI). Brain Res. 576, 271–276.
26. Tanno, H., Nockels, R.P., Pitts, L.H., and Noble, L.J. (1992). Breakdown of the blood-brain barrier after fluid percussive brain injury in the rat. Part 1: distribution and time course of protein extravasation. J. Neurotrauma 9, 21–32.
27. Barzo, P., Marmarou, A., Fatouros, P., Corwin, F., and Dunbar, J. (1996). Magnetic resonance imaging-monitored acute blood-brain barrier changes in experimental traumatic brain injury. J. Neurosurg. 85, 1113–1121.
28. Chavko, M., Prusaczyk, W.K., and McCarron, R.M. (2006). Lung injury and recovery after exposure to blast overpressure. J. Trauma 61, 933–942.
29. Vieira, P. and Rajewsky, K. (1988). The half-lives of serum immunoglobulins in adult mice. Eur. J. Immunol. 18, 313–316.
30. Wolman, M., Klatzo, I., Chui, E., Wilmes, F., Nishimoto, K., Fujiwara, K., and Spatz, M. (1981). Evaluation of the dye-protein tracers in pathophysiology of the blood-brain barrier. Acta Neuropathol. 54, 55–61.
31. Maxwell, W.L., Whitfield, P.C., Suzen, B., Graham, D.I., Adams, J.H., Watt, C., and Gennarelli, T.A. (1992). The cerebrovascular response to experimental lateral head acceleration. Acta Neuropathol. 84, 289–296.
32. Adams, J.H., Graham, D.I., and Gennarelli, T.A. (1981). Acceleration induced head injury in the monkey. II. Neuropathology. Acta Neuropathol. Suppl. 7, 26–28.
33. Gennarelli, T.A., Adams, J.H., and Graham, D.I. (1981). Acceleration induced head injury in the monkey.I. The model, its mechanical and physiological correlates. Acta Neuropathol. Suppl. 7, 23–25.
34. Gennarelli, T.A., Thibault, L.E., Adams, J.H., Graham, D.I., Thompson, C.J., and Marcincin, R.P. (1982). Diffuse axonal injury and traumatic coma in the primate. Ann. Neurol. 12, 564–574.
35. Raghupathi, R., Margulies, S.S. (2002). Traumatic axonal injury after closed head injury in the neonatal pig. J. Neurotrauma 19, 843–853.
36. Gutierrez, E., Huang, Y., Haglid, K., Bao, F., Hansson, H.A., Hamberger, A., and Viano, D. (2001). A new model for diffuse brain injury by rotational acceleration: I model, gross appearance, and astrocytosis. J. Neurotrauma 18, 247–257.
37. Davidsson, J. and Risling, M. (2011). A new model to produce sagittal plane rotational induced diffuse axonal injuries. Front. Neurol. 2, 41.
38. Fijalkowski, R.J., Stemper, B.D., Pintar, F.A., Yoganandan, N., Crowe, M.J., and Gennarelli, T.A. (2007). New rat model for diffuse brain injury using coronal plane angular acceleration. J. Neurotrauma 24, 1387–1398.
39. Goldstein, L.E., Fisher, A.M., Tagge, C.A., Zhang, X.L., Velisek, L., Sullivan, J.A., Upreti, C., Kracht, J.M., Ericsson, M., Wojnarowicz, M.W., Goletiani, C.J., Maglakelidze, G.M., Casey, N., Moncaster, J.A., Minaeva, O., Moir, R.D., Nowinski, C.J., Stern, R.A., Cantu, R.C., Geiling, J., Blusztajn, J.K., Wolozin, B.L., Ikezu, T., Stein, T.D., Budson, A.E., Kowall, N.W., Chargin, D., Sharon, A., Saman, S., Hall, G.F., Moss, W.C., Cleveland, R.O., Tanzi, R.E., Stanton, P.K., and McKee, A.C. (2012). Chronic traumatic encephalopathy in blast-exposed military veterans and a blast neurotrauma mouse model. Sci. Transl. Med. 4, 134ra160.
40. Long, J.B., Bentley, T.L., Wessner, K.A., Cerone, C., Sweeney, S., and Bauman, R.A. (2009). Blast overpressure in rats: recreating a battlefield injury in the laboratory. J. Neurotrauma 26, 827–840.
41. Svetlov, S.I., Prima, V., Kirk, D.R., Gutierrez, H., Curley, K.C., Hayes, R.L., and Wang, K.K. (2010). Morphologic and biochemical characterization of brain injury in a model of controlled blast overpressure exposure. J. Trauma 69, 795–804.
42. Kaur, C., Singh, J., Lim, M.K., Ng, B.L., Yap, E.P., and Ling, E.A. (1995). The response of neurons and microglia to blast injury in the rat brain. Neuropathol. Appl. Neurobiol. 21, 369–377.
43. Algattas, H. and Huang, J.H. (2014). Traumatic Brain Injury pathophysiology and treatments: early, intermediate, and late phases post-injury. Int. J. Mol. Sci. 15, 309–341.
44. Chodobski, A., Zink, B.J., and Szmydynger-Chodobska, J. (2011). Blood-brain barrier pathophysiology in traumatic brain injury. Transl. Stroke Res. 2, 492–516.
45. Lozano, D., Gonzales-Portillo, G.S., Acosta, S., de la Pena, I., Tajiri, N., Kaneko, Y., and Borlongan, C.V. (2015). Neuroinflammatory responses to traumatic brain injury: etiology, clinical consequences, and therapeutic opportunities. Neuropsychiatr. Dis. Treat. 11, 97–106.
46. Effgen, G.B., Vogel, E.W., 3rd, Lynch, K.A., Lobel, A., Hue, C.D., Meaney, D.F., Bass, C.R., and Morrison, B., 3rd. (2014). Isolated primary blast alters neuronal function with minimal cell death in organotypic hippocampal slice cultures. J. Neurotrauma 31, 1202–1210.
47. Wang, Y., Wei, Y., Oguntayo, S., Wilkins, W., Arun, P., Valiyaveettil, M., Song, J., Long, J.B., and Nambiar, M.P. (2011). Tightly coupled repetitive blast-induced traumatic brain injury: development and characterization in mice. J. Neurotrauma 28, 2171–2183.
48. Duckworth, J.L., Grimes, J., and Ling, G.S. (2013). Pathophysiology of battlefield associated traumatic brain injury. Pathophysiology 20, 23–30.
49. Vandevord, P.J., Bolander, R., Sajja, V.S., Hay, K., and Bir, C.A. (2012). Mild neurotrauma indicates a range-specific pressure response to low level shock wave exposure. Ann. Biomed. Eng. 40, 227–236.
50. Arun, P., Abu-Taleb, R., Oguntayo, S., Tanaka, M., Wang, Y., Valiyaveettil, M., Long, J.B., Zhang, Y., and Nambiar, M.P. (2013). Distinct patterns of expression of traumatic brain injury biomarkers after blast exposure: role of compromised cell membrane integrity. Neurosci. Lett. 552, 87–91.

Address correspondence to:
Barclay Morrison III, PhD
Columbia University
Department of Biomedical Engineering
351 Engineering Terrace, MC8904
1210 Amsterdam Avenue
New York, NY 10027

E-mail: bm2119@columbia.edu